Journal of the Korean Society of Remote Sensing, Vol. 10, No. 2, 1994

JERS-1 SAR DATA CHARACTERISTICS FOR GEOLOGICAL APPLICATIONS

Wooil M. Moon*, Bo Li*, J.S. Won, H.W. Yoo**, V. Singhroy*** and Y. Yamaguchi****

* The University of Manitoba, Winnipeg, Canada R3T 2N2
** Korea Ocean Research and Development Institute, P.O. Box 29, Ansan, Korea
*** Canada Center for Remote Sensing, Ottawa, Canada K1A 0Y7
**** Geological Survey of Japan, 1-1-3 Higashi, Tsukuba, Ibaraki 305, Japan

Abstract

The JERS-1 is an Earth Resources Satellite launched by NASDA (National Space Development Agency) of Japan, in February in 1992 and has two sensors; SAR (L - Band Synthetic Aperture Radar) and OPS (SWIR and VNIR radiometers). In this research note, the basic properties and data characteristics of the SAR data are summarized based on the observations made on the data sets received for the Nahanni Canadian test site, Northwest Territories. The JERS-1 SAR data quality, including the spatial resolution of the data, is, in general, excellent for most geological applications.

Introduction

Geological application of SAR (Synthetic Aperture Radar) system has rapidly become very popular in many Earth Science sub-disciplines such as lithological mapping, structural geology mapping, non-renewable resource exploration, geomorphology, glacial geology, water resources development, natural disaster monitoring and prediction, environmental science, and Earth observation studies (NASA, 1988; Li, 1993; Singhroy et al., 1993). Usefulness and effectiveness of the SAR sensors are expected to be greatly increased as new technological advances, such as increasing spatial resolution and multiple frequency

and multiple polarization imaging capabilities, become available. Furthermore, active research on new data processing and imaging techniques, such as inversion and imaging of the geophysical properties of the Earth's surface materials directly from backscattered SAR wavefields (Moon, 1991; Won and Moon, 1992) is expected to open more application developments for space-borne SAR systems such as RADARSAT (to be launched in 1995 by the Canadian Space Agency).

Orbit and Platform Characteristics of JERS-1

There are presently two Earth resources satellites, ERS-1 and JERS-1, with SAR imaging systems in operation. The orbital and sensor characteristics of the JERS-1 will be discussed with specific point by point comparison with the CCRS's airborne C-SAR and ERS-1 SAR system. The ERS-1 was launched in July 1991 and the JERS-1 in February 1992. Some of the orbit and platform characteristics of these two satellite sensors are listed in Table 1 (CCRS, 1992; NASDA, 1990) along with CCRS's airborne SAR system which was made available for various application studies in Canada over a number of test sites.

Table 1. General specification of the JERS-1 SAR system and orbit parameters.

Parameters	CCRS's C-SAR	ERS-1 SAR	JERS-1 SAR
Altitude	6.76km	782km	568km
Resolution (row x pixel)	6.9m x 15m	12.5m x 12.5m	12.5m x 12.5m
Wave band	C (/X) (5300MHz)	C (5300MHz)	L (1275MHz)
Polarization	HH (VV, HV,VH)	VV	HH
Swath width	20 - 64km	100km	75km
Repeat period (cycle)	n.a.	35 (3/180) days	44 days

Even though all SAR systems, in principle, have day/night and all weather observation capabilities, actual usefulness and effectiveness of the system very much depends on the available wave bands and polarization. For geological application of the SAR system over

an area with heavy vegetation cover, longer wave length is preferred due to its penetration capability and volume scattering characteristics.

As for the polarization of the wavefield, application suitability of specific polarization is very much case dependent and further study is need for geological applications.

SAR Sensor and Data Characteristics

Most geological applications of SAR data, except direct inversion of the backscattered wavefield, depend critically on the frequency, polarization, spatial resolution, look direction, incidence angle, swath width, and processed image depth. The major difference between the ERS-1 and JERS-1 SAR system is the frequency (wave band) of the signal wavefield. With longer wavelength of L-Band, JERS-1 SAR data is expected to have better penetration capability than the ERS-1 SAR system. This will benefit geological investigation in both barren and heavily vegetated areas. Even though the ground penetration will be very limited, depending on the moisture content of the study area, imaged backscattered wavefields will include volume scattering and represent the shallow subsurface geological information.

The look angle of a SAR system plays an important role in SAR image characteristics. The altitude of the SAR sensors have a significant effect on local incidence angles and on the final image products. Both ERS-1 and JERS-1 platforms have very high altitude, compared with CCRS's airborne SAR system, and distortions in image products due to surface topography are largely reduced. In mountainous areas such as the Nahhani study area, large shadows from rugged terrain make the airborne C-SAR difficult to use, requiring additional processing.

There are several types of SAR image products available from each sensor, and they differ mainly in pixel resolution and the geometrical corrections applied. For the end user, it is, however, not necessary to know all the processing details. The main characteristics of the three sets of SAR image being described and compared are summarized in Table 2.

Both ERS-1 and JERS-1 SAR data products used the UTM map projection and the projection results are, in general, acceptable in the areas where the terrain is relatively flat. In very mountaineous regions, however, the image distortion becomes a serious problem. The mountain ridges, in the study area, lean foward to the sensors and create distorted image impressions. This phenomenon is more serious with the ERS-1 SAR data than

those of the JERS-1 image. On CCRS's C-Band SAR image, the topographic relief produced large shadows due to the very low altitude of the SAR platform, compared with the satellite platforms. Multi-look techniques have been utilized to reduce the speckle noise in all three SAR images. With the number of looks being seven and six, the CCRS's C-Band SAR and ERS-1 SAR images appear smooth and less noisy, whereas the JERS-1 SAR images have a much higher level of speckle because of fewer number of looks (three) and the lower signal frequency (L-Band). The JERS-1 satellite also suffered technical problems during the commissioning period, resulting in lower power in the SAR antenna and subsequently resulting in lower S/N ratio in the SAR image data).

Table 2. Specifications of the JERS-1 SAR image products compared to the CCRS's C-SAR and ERS-1 SAR data.

Parameters	CCRS's C-SAR	ERS-1 SAR	JERS-1 SAR
Byte/pixel	1	1	2
Map Projection	n.a.	UTM	UTM
Corrections Applied	n.a.	Precision Geocoded	Geocoded
Scene dimension (lines x pixels)	22,650 x 4096	4432 x 8000	6400 x 6000
Number of Looks	7	6	3
Azimuth	~ 85°	~ 261.5°	~ 278°
Incidence angle at mid-swath	n.a.	23.5°	35°
Date of Data Acquisition	1989-05-09 (17:23:19)	1992-10-17 (19:29:18)	1993-07-18 (19:18:07)
Auxiliary Information	n.a.	Image Data Histogram file	Coordinate Conversion file

The experimental study area, Nahanni earthquake area, is centered at N62° 16′, W124° 30′ and covers an area of approximately 50.6 km x 37.5 km. The images from the ERS-1, JERS-1 and CCRS's airborne C-SAR are shown in Figure 1. All three images are processed using spatial filtering and histogram equalization for signal enhancement and noise reduction.

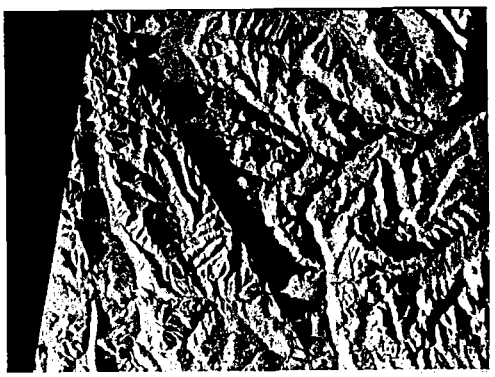

(a)

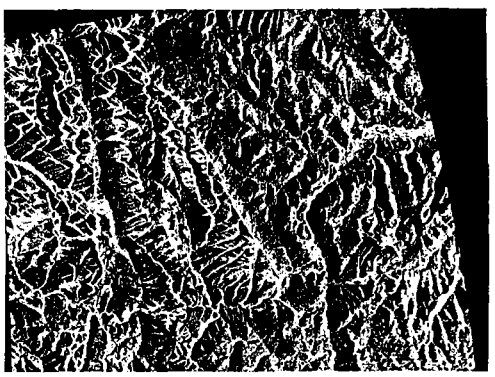

(b)

(c)

Figure 1. (a) CCRS's airborne C-Band (HH) SAR image over Nahanni test site.
(b) ERS-1 C-Band (VV) SAR image over Nahanni test site.
(c) JERS-1 L-Band (HH) SAR image over Nahanni test site.

There are no significant differences between the ERS-1 and JERS-1 image products in spite of the fact that they were acquired with quite different signal frequencies. If the readers are interested in the details of the raw data products, they are listed in Table 3. The statistical data in Table 3 represent only a small test area with 90,000 pixels and it reflects image formation algorithms more than the actual image data. Nevertheless, these parameters and the frequency of pixel value plots shown in Figure 2 may be useful to some of the JERS-1 data users.

Table 3. Statistical characteristics of the raw JERS-1 and ERS-1 SAR data pixel values.

Parameters	JERS-1 SAR	ERS-1 SAR
Mean pixel values (in 8 bit image field)	29.06	63.91
s2	14.04	34.26

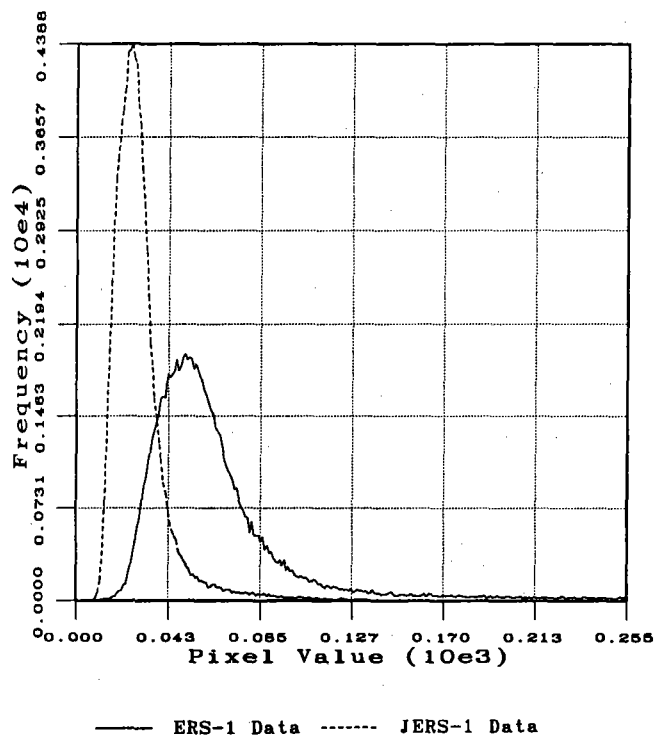

Figure 2. Histogram plot of the raw JERS-1 and ERS-1 SAR data pixel values.

The real difference may, however, become important in certain applications such as in the inversion of the SAR data for specific geophysical parameters. The gray level differences, which might have been caused either by seasonal differences in soil moisture and the surface vegetation cover (the ERS-1 data was recorded in October and the JERS-1 image in July) or by the processing algorithm should be taken seriously if the data were to be used without inversion processing. The low mean value and the narrow standard deviation of the JERS-1 data indicate that it will be necessary for any practical application that some preprocesing, including contrast stretching, be carried out.

In addition to the actual image data, both ERS-1 and JERS-1 CCT data tapes contain auxiliary data records. In the case of the ERS-1/SPG product tape, a histogram table is included in the SAR trailer file. This table contains the pixel number counts corresponding to grey levels 0 to 255. This table can be very useful in SAR image processing, such as histogram equalization and linear grey level stretching with high and low-cut-off points. To locate certain targets on an image accurately, it is sometimes desirable to convert the coordinates between the image coordinate (row, column) and the geographic coordinate (longitude, latitude). This task involves selection of control point pairs on both the SAR image and the base map (a topographic sheet), which can then be matched using a least squares approximation method. The JERS-1/2.1 data tapes provide the user with the coordinate conversion coefficients in the SAR leader file to allow convenient conversion from the image coordinates (row, column) to the geographic coordinate (Easting, Northing) and vice versa. The coordinate conversion formula given is as follow :

$$E = a_{11} + a_{12} \times L + a_{13 \times P} + a_{14} \times L \times P$$
$$N = a_{21} + a_{22} \times L + a_{23 \times P} + a_{24} \times L \times P$$

and,

$$L = b_{11} + b_{12} \times L + b_{13 \times P} + b_{14} \times L \times P$$
$$P = b_{21} + b_{22} \times L + b_{23 \times P} + b_{24} \times L \times P \text{ ,}$$

where N and E denote the Easting and Northing in degrees and L and P denote the line and pixel numbers (RESTEC, 1992).

Notes on JERS-1 SAR Image Processing

One of the first concerns in JERS-1 SAR image processing involves speckle reduction,

which may be accomplished by a filtering technique, either in spatial filtering or in frequency filtering (Touzi and Lopes, 1993). Both spatial and frequency filtering techniques are tested in this research with the JERS-1 SAR data. Several trials with different parameters indicate that the low-pass frequency filtering produced an acceptable final smoothed image, suppressing high frequency speckle noise while maintaining the essential image details. A drawback of this approach is large amount of computation needed in both FFT and IFFT steps. A more economical approach is to use simple box-car filters in the spatial domain. Several image enhancement methods were preliminarily tested with the JERS-1 SAR data. It appears the histogram equalization is more effective for the JERS-1 SAR image than the straight linear stretching or simple moving window based enhancement techniques. The optimum result was obtained with a successive application of a spatial filtering technique, followed by the histogram equalization.

On the JERS-1/2.1 SAR data tape, each pixel value occupies two bytes. This allows a wider dynamic range for the final SAR image. However, the histogram of the JERS/2.1 data shows that the pixel values of the image spread more or less evenly over the whole range. In case the workstation monitor can display only one byte (8 bit) image, the two byte (16 bit) image data must be truncated to be converted into one byte prior to actual display. One of the methods which can be used for compressing two byte information to one byte data may be accomplished using a relathionship

$$\max\left(\int_{2j}^{2j+8} p(i)\, di \right)$$

where $p(i)$ is the probability density function for pixel grey level i, $2j$ and $2j+8$ are the integral range which will maximize the integral. (Here the integration variable i and j are considered to have continuous values whereas the same i and j in the following summation equation are discrete). In the case of SAR image data, all the grey levels are discrete values and the maximization process may be simplified as

$$\max\left(\sum_{i=2j}^{2j+8} h(i) \right),$$

where $h(i)$ is the frequency count in the histogram for grey level i, and $[2j, 2j+8]$ is the range for the summation which will maximize the summation results (Hall, 1979). The experiment shows that $j = 6$ gives the best result, which means that the resulting one-byte pixel value retains the original 6th bit up to the 13th bit information.

Conclusions

The preliminary information, learned from the JERS-1 SAR image data over the Nahanni Canadian test site, is summarized in this paper for other investigators who might be interested in JERS-1 SAR data for geological applications.

Compared to the CCRS's C-Band SAR data, the JERS-1 SAR image has less foreshortening or layover and thus can provide a more comprehensive view of geological structures. In terms of geometric distortion due to terrain relief, the JERS-1 image is better than ERS-1 image, and the JERS-1 image data is more suitable for robust applications where the geographic accuracy is high.

Imaging parameters of the JERS-1 SAR system, L - Band (23 cm wavelength) and HH polarization are adequate for most geological applications. The L-Band speckle effects of the JERS-1 image data is greater than those of the CCRS's airborne and ERS-1 SAR image data. This L-Band data should provide more useful information for evaluating the nature of weathering and mass wasting of geological materials in general. For quick robust structural applications, the speckle problem may be reduced by applying a low pass frequency filter. According to the NASA EOS Instrument Panel Report on SAR, the highest priority frequency for soil erosion investigation was, in fact, the L-Band followed by the C-Band and the new JERS-1 data should provide important information for specific applications. Both the VV and HH polarizations of the ERS-1 and JERS-1 SAR data should be useful for the majority of structural geological terrains. The HH polarization has been slightly favored, however, simply because of its enhanced ability to penetrate thin low loss mantles of sand, snow, ice, and most geological materials. To take real advantage of the imaging parameters of the JERS-1, however, it would be necessary to develop rigorous direct inversion techniques for specific geophysical parameters.

The auxiliary file on the image- and geographic- coordinate conversion coefficients, included with the JERS-1/2.1 data tape, allows the end user to quickly convert the image- and geographic coordinates.

Acknowledgments

This research is funded by an NSERC operating grant A-7400 to W. M. Moon. The JERS-1 Data sets were provided by the RESTEC of Japan as a part of the JERS-1 SAR

science verification program # 0202. The ERS-1 SAR data for this research was kindly supplied by Dr. Bob O'Neil (Major Projects Office) of CCRS and the CCRS's airborne C-Band SAR data tapes were provided for this project as a part of the RDDP agreement.

References

CCRS. 1992. "RS-1 Canadian User Guide", Canada Center for Remote Sensing.

Hall, E.L., 1979. "Computer Image Processing and Recognition", Academic Press, New York.

Li, B., 1993. "Application of Remote Sensing Techniques for the Seismo-tectonic Study of Nahanni Earthquake Area", M.Sc. Thesis, The University of Manitoba, Canada.

Moon, W.M., 1991. "Born Inversion of surface scattered SAR Wavefield", *Canadian Journa l of Physics*, Vol. 69, pp. 1256-1260.

NASA. 1988. "Earth Observation System - Instrument Panel Report", Volume IIf, SAR. (Ed itor - K.R. Carver).

NASDA. 1990. "Earth Resources Satellite-1", RESTEC/NASDA, Japan.

RESTEC. 1992. "User's Guide for JERS-1 SAR Data Format", Earth Observation Center, H iki-gun, Saitama-ken, Japan.

Singhroy, V., R.V. Slaney, P. Lowman, Jr., J. Harris, and W.M. Moon. 1993. "RADARSAT and Radar Geology in Canada", *Canadian Journal of Remote Sensing*, Vol. 19, pp. 33 8-351.

Touzi, R., and A. Lopes, 1993. "Analysis of Speckle Filtering in Polarimetric SAR imagery", Proceedings of IGARSS '93, Vol., III, pp. 1419-1422.

Won, J.S., and W.M. Moon. 1992. "Inversion of SAT Data for Surface Scattering", *Geophys ical Journal (International)*, Vol. 108, pp. 423-432.